New variable low-temperature scanning tunneling microscope for use in ultrahigh vacuum

A. R. Smith and C. K. Shih
Department of Physics, University of Texas, Austin, Texas 78712

(Received 11 July 1994; accepted for publication 15 November 1994)

We describe the design and characterization of a new variable low-temperature scanning tunneling microscope (STM) which has been proven to give atomic resolution at temperatures between 77 K and room temperature but which is also capable of performing experiments as low as 4 K. The STM "head" itself consists of a unique cold dewar made up of an upper and lower reservoir connected together by two tubes which pass through an 8 in. conflat flange. The STM stage is suspended in between the two reservoirs by three long springs which pass through holes in the upper reservoir and also attach to the top flange. An adjustable cold shroud surrounds the STM stage for radiation shielding while allowing sample and tip transfer when raised. It has the additional advantage of providing a controllable heat leak. By raising the shroud, the temperature can be increased; by lowering it, the temperature can be decreased. The cold reservoirs can be filled with either liquid nitrogen or liquid helium. In the case of liquid helium, an additional liquid nitrogen "jacket" surrounds the STM head. Everything is operated inside a customized ultrahigh vacuum chamber containing low-energy electron diffraction and various sample preparation facilities. A detailed description of the STM is presented together with performance results. © *1995 American Institute of Physics.*

I. INTRODUCTION

Since the invention of scanning tunneling microscopy (STM),[1] there has been a great deal of interest in developing variable-temperature STM. While some microscopes have been designed to work at around or above room temperature, of particular interest has been the development of STMs which operate at low temperatures, namely at liquid nitrogen or liquid helium temperatures.[2–7] A number of low-temperature STMs have been designed for use in ultrahigh vacuum (UHV).[8–11] Three important reasons for doing UHV STM at variable and/or low temperatures are the following: first, to investigate temperature-dependent phase transitions at the atomic scale; second, to study atomic dynamics in a temperature regime where the atomic processes are slowed down; third, to study novel quantum phenomena which either exist only at low temperature or are best seen at low temperature. An example of phase transitions studied at low temperature would be work done by Wolkow on Si(100) 2×1.[12] Wolkow is also studying the atomic kinetics of Si atoms on the same surface while Eigler *et al.* used a low-temperature STM to manipulate and image individual xenon atoms on a Ni (110) surface.[13] Regarding studies of novel quantum phenomena at low temperatures, Crommie *et al.* have imaged two-dimensional electron standing waves on a Cu (111) surface and created the first "quantum corrals."[14] Our low-temperature UHV STM has been designed with the capability of performing similar investigations to those named above but with an additional important motivation in mind, namely, the study of low-dimensional quantum heterostructures. This involves studying the UHV-cleaved cross-sectional surfaces of semiconductor heterostructures and is an important extension of the currently growing field of cross-sectional STM.[15–20] To perform such an investigation, it is essential to have a two-dimensional translation stage which is free of backlash and crosstalk if one is to be able to position the STM tip within the epilayer region which contains the heterostructures of interest. To achieve this requirement, our STM makes use of a two-dimensional piezoelectrically driven translation system which not only meets the high precision requirements but also performs well at low temperatures.[21]

II. INSTRUMENT DESCRIPTION

Shown in Fig. 1(a) is a cross-cut sideview of the low-temperature STM mounted inside the liquid nitrogen jacket. The liquid helium reservoir (composed of an upper and lower reservoir connected by the fill tubes) is built into the UHV chamber by means of two 1/2 in. stainless steel tubes which pass through an 8 in. conflat flange. The liquid nitrogen jacket is also built into the UHV chamber but is a completely separate piece. In Fig. 1(a), the jacket is shown in lighter shading and can be removed when not needed. The STM stage is composed of an aluminum disc with a copper bottom (approximate weight of stage is 1 kg) and is suspended between the upper and lower reservoirs by three long springs passing through holes in the upper reservoir and connecting to fixed points at the top flange. The main components of the STM are mounted rigidly on the stage and consist of a quadrant-type piezoelectric scanner with the tip and a two-dimensional walker[21] with the sample. The long soft springs make it possible to reduce the vibrational noise due to bubbling of the liquid nitrogen and other vibrational noise sources. Further, being made of stainless steel and having a relatively small total cross-sectional area, these springs present very little undesirable conductive heating to the sample stage. Eddy current damping for the system is provided by aluminum rings which are mounted to the lower reservoir as seen in Fig. 1(b) and damping magnets which

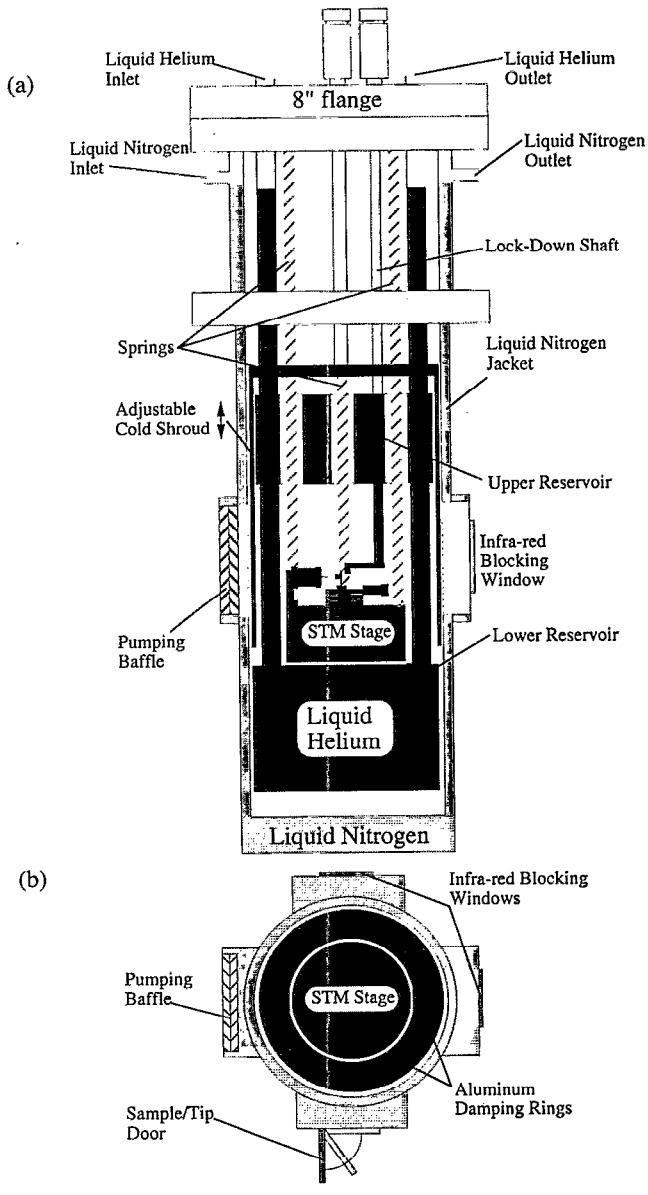

FIG. 1. Design of UHV STM system showing the low-temperature microscope (darker shading) mounted inside the optional liquid nitrogen jacket (lighter shading). For studies at liquid helium temperature, the nitrogen jacket acts as a radiation shield. For studies at liquid nitrogen temperatures, this jacket can be removed. (a) cross-cut view from the side showing the adjustable cold shroud, and (b) cross-cut view from the top showing the externally actuated tip/sample transfer door and the aluminum damping rings.

are imbedded in the sides of the STM stage. During cooldown, the springs contract by about 1/4 in.; however, vibration isolation is unaffected due to the large effective range of the damping mechanism.

The electrical wires feed through the top flange and reach the STM stage region after passing through a thin tube which itself slides through a special hole in the upper reservoir. The electrical wires branch out to fixed points connected to the bottom reservoir and are then looped over to the STM stage, providing a soft connection for very small vibrational noise coupling. This tube serves a second important function. As it is essential to be able to lock the walker

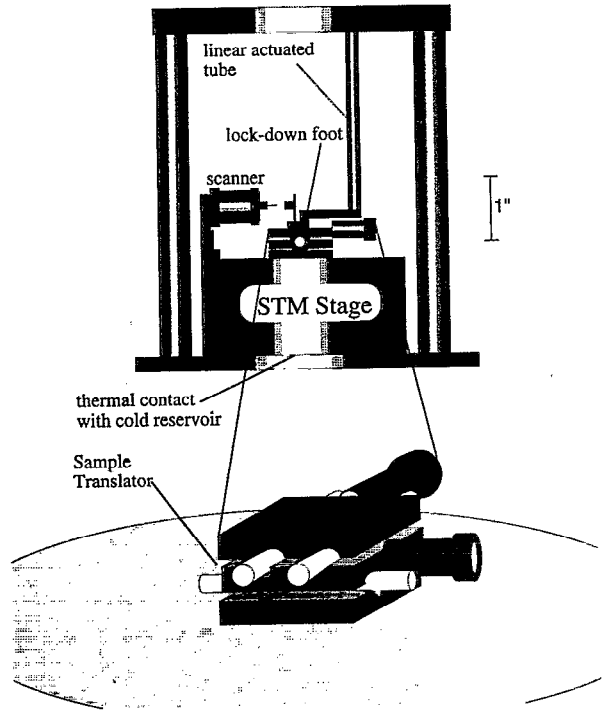

FIG. 2. Zoom-in view of the central parts of the STM, showing the lock-down mechanism and the two-dimensional sample translator used especially in cross-sectional studies.

in place in order to transfer samples, it is equally necessary to have good thermal contact with the lower reservoir during the initial cooldown. Further, it is convenient to be able to conductively cool the STM stage while allowing the walker freedom of motion. These desirable features prompted the design of a two-phase lock-down foot which is attached to the bottom of the same tube through which the electrical wires pass. This tube is attached to a linear feedthrough at the top flange and can be moved up and down. Extra length in the electrical wires allows enough "play" for this to occur. In the first lock-down phase, only the STM stage is pressed down to the lower reservoir by two spring-loaded foot pads; the walker is still free to move. In this phase, tip transfer is allowed but not sample transfer. In the second lock-down phase, a third foot pad presses down on the sample mover, locking it in place, and allowing samples to be transferred.

The sample translation system used in this STM[21] (developed in our laboratory) is depicted together with the STM stage in its fully locked position in Fig. 2. The translator consists of two orthogonal, piezoelectrically driven walkers, the second walker riding on top of the first. The driving piezos are made of PZT-4.[22] The walkers can be moved over macroscopically large distances in the horizontal plane but also have a very fine step size and so are used for course approach and lateral translation. Further, the walker system has been found to be essentially free of backlash and crosstalk, making it the ideal sample translator for use in cross-sectional STM studies.

The piezoelectric material used for the scanner in this STM is also made of PZT-4. For this material, the response coefficient d_{31} varies with temperature in a qualitatively dif-

ferent manner over the temperature range 4–300 K than either PZT-5A or PZT-5H. Whereas the coefficients for each of these latter two decrease with decreasing temperature, for PZT-4, the coefficient first increases (with decreasing temperature) approximately 8%, reaching its maximum at about 235 K, levels off, then begins to decrease with decreasing temperature at about 200 K.

Sample and tip transfer is extremely straightforward. These operations are achieved with the use of a specially designed manipulator jaw which works by an opening/closing two-finger mechanism. The jaw grabs both samples and tips, moves them between the STM and a sample/tip garage, and also has sample heating capability. Samples can be either mounted in a holder such as in cross-sectional studies or can be wafer-type samples such as in Si/Ge studies—the STM sample stage can accommodate either sample type.

Radiation heating is reduced to a minimum by the use of an aluminum cold shroud [Fig. 1(a)] which can be externally actuated to move up and down. In its up position, it allows complete optical and mechanical access to the STM for tasks such as sample and tip loading and positioning. In its down position, it is pressed solidly onto the top cold reservoir which then cools the sides of the shroud, providing for the heat shielding. The only heat leaks remaining are the small holes in the upper cold reservoir through which the springs pass. In-between positions of the cold shroud allow whatever amount of radiation heating is needed in order to restabilize the STM to any desired temperature. In addition, at a unique intermediate position, a small aperture in the cold shroud is aligned with the sample, allowing evaporation at low temperatures while the rest of the STM is still well shielded.

An important advantage of this design is its modularity. While all UHV STMs capable of operation at liquid helium temperature require the use of a double dewar, this design allows the outer dewar to be removed making this into a room-liquid nitrogen temperature STM. Removal of the outer dewar can be accomplished easily and makes STM operation as simple as any room-temperature STM. Such a modular design provides a great deal of versatility.

III. PERFORMANCE RESULTS

Thus far, we have performed all of our low-temperature testing without the liquid nitrogen jacket and by filling the inner reservoirs with only liquid nitrogen. The temperature was measured using a chromel-alumel thermocouple at the point of the sample. We estimate this measurement to be accurate to within ±2 K down to about 80 K; below this temperature, a more suitable temperature probe will be required.

The cooling rate of this STM occurs in two fairly distinct phases. During the first phase, the temperature decreases rapidly due to the good thermal conductivity between the STM stage and the cold reservoir when the stage is pressed down into thermal contact with the cold reservoir. In this way, the sample temperature reaches 120 K within 3 h. The next phase of cooling takes an additional 3–5 h in order to reach 80 K. This phase is characterized by the greater role played by radiative cooling.

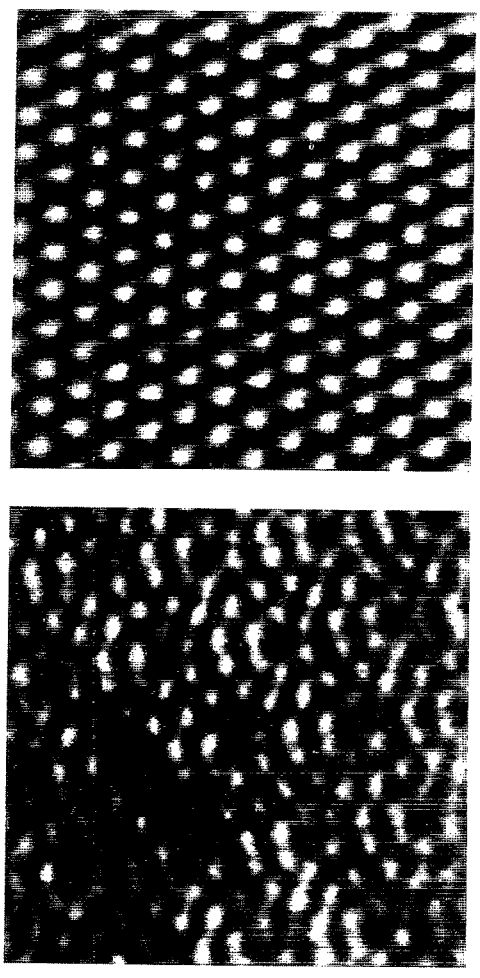

FIG. 3. Room-temperature atomic resolution images of graphite and Si(111) 7×7. For graphite, the scan area is 24 Å×24 Å with a corrugation amplitude of 0.9 Å acquired with a sample bias of 0.21 V. For Si, the scan area is 71 Å×71 Å with a maximum corrugation amplitude of 0.18 Å acquired at a sample bias of 2.92 V.

To characterize this STM, we first tested it using graphite and Si(111) 7×7. Shown in Fig. 3 are room-temperature atomic resolution STM images of these surfaces acquired with our STM. While we have also performed low-temperature studies of each of these, here we will present only our initial low-temperature results on the UHV-cleaved GaAs(110) surface. Shown in Figs. 4(a)–4(c) are three constant current, atomic resolution STM images of the GaAs(110) surfaces at 300, 235, and 200 K, respectively. There is nothing particularly special about the choice of these temperatures; due to the STM shutter design, such images can be acquired at any temperature desired by simply adjusting the thermal leak using the cold shroud. Stabilization at a given temperature can be reached within 10 min.

The atomic row spacings in these images were used to check the temperature dependence of the piezocalibration. After reducing the temperature from 300 to 235 K, the apparent spacing between atomic rows decreased by about 8%, in good agreement with the expected temperature dependence of d_{31} for PZT-4. After decreasing the temperature further to 203 K, the apparent row spacing increased only slightly, also in good agreement with the expected behavior.

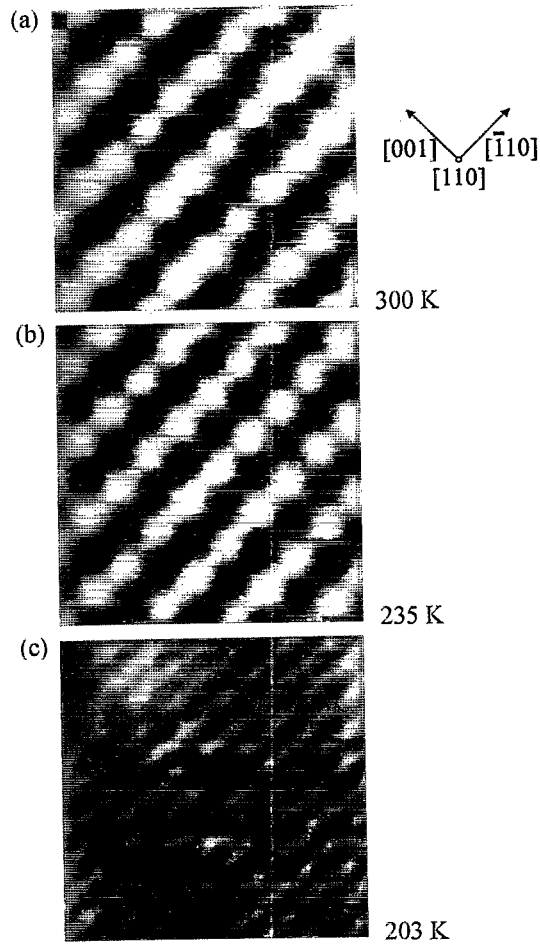

FIG. 4. Atomic resolution images of the GaAs (110) surface at different temperatures. (a) 25 Å×25 Å scan size, corrugation amplitude 0.16 Å, and sample bias −1.92 V at 300 K (b) 25 Å×25 Å scan size, corrugation amplitude 0.18 Å, and sample bias 2.59 V at 235 K, (c) 50 Å by 50 Å scan size, corrugation amplitude 0.28 Å, and sample bias 2.59 V at 203 K.

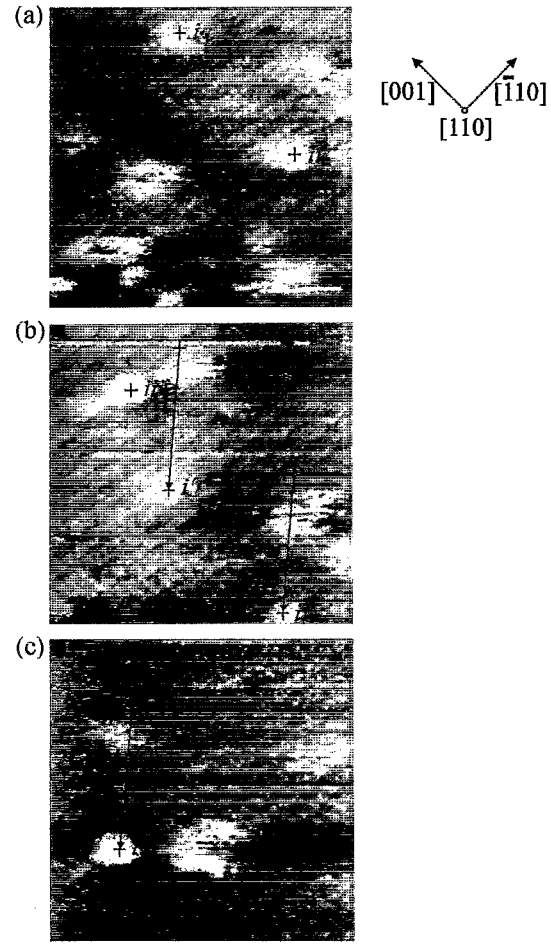

FIG. 5. Time sequence of 100 Å by 100 Å images of the GaAs (110) surface at 237 K, acquired about 48 s apart at a sample bias of 2.59 V. Sample drift is observed as an apparent shift in the positions of features i, ii, and iii to their new positions in the next consecutive image i′, ii′, and iii′, indicated by the arrows.

In order to perform temperature-dependent studies of surfaces, it is important that the STM be reasonably stable against thermal drift during the time that the temperature is changing. In order to determine the amount of thermal drift present in this STM, we allowed it to warm up slowly while simultaneously acquiring STM images. Doing so allowed us to directly observe the apparent drifting speed for a given rate of temperature change. Shown in Figs. 5(a)–5(c) is a sequence of three images of the UHV-cleaved GaAs (110) surface at 237 K. Due to the tip condition, the atomic corrugation in these images is extremely weak. However, since we know the scan rate, the number of scan lines per image, and the total amount of time required to acquire and save an image before beginning the next, it is possible to deduce the apparent drift speed by using fixed reference points on the surface from one image to the next. In this case, the scan rate was 3 Hz, the image contained 128 scan lines, and the total amount of time required to acquire and save an image was about 48 s. Therefore, by measuring the apparent shift in the position of feature i, for example, between images (a) and (b) (denoted in the figure as an arrow to its new position i') and calculating the elapsed time between scanning over this feature in the two consecutive images, we calculate the apparent drifting speed to be about 100 Å/min at 237 K with a warming-up rate of about 4 K/h. We have also performed a similar study at a lower temperature of 120 K where the temperature was increasing at about 2 K/h. Repeating the calculation as before for a surface feature and adjusting for the reduction in the piezocoefficient, we conclude that the apparent drift speed is about 34 Å/min at this temperature, roughly one-third of that at the higher temperature but at half the warming-up rate. For purposes of temperature-dependent STM studies, such a low thermal drift rate will be quite adequate.

Finally, experiments using liquid helium are underway to verify operation at liquid helium temperatures.

ACKNOWLEDGMENTS

The authors would like to thank Ping Meng, who helped during the construction phase of this instrument and Dr. Shang-Jr Gwo, who helped during the initial testing phase. Special thanks also go to Les Deavers and the other expert machinists in the UT Physics department who built the major

parts of this equipment and to Edward McKnight for many valuable discussions on instrument design and construction.

[1] G. Binnig and H. Rohrer, Phys. Rev. Lett. **49**, 57 (1982).
[2] Douglas P. E. Smith and Gerd Binnig, Rev. Sci. Instrum. **57**, 2630 (1986).
[3] A. P. Fein, J. R. Kirtley, and R. M. Feenstra, Rev. Sci. Instrum. **58**, 1806 (1987).
[4] J. W. Lyding, S. Skala, J. S. Hubacek, R. Brockenbrough, and G. Gammie, Rev. Sci. Instrum. **59**, 1897 (1988).
[5] Jurgen Burger, S. C. Meepagala, and E. L. Wolf, Rev. Sci. Instrum. **60**, 735 (1989).
[6] D. N. Davydov, R. Deltour, N. Horii, V. A. Timofeev, and A. S. Grokholski, Rev. Sci. Instrum. **64**, 3153 (1993).
[7] I. B. Altfeder and A. P. Volodin, Rev. Sci. Instrum. **64**, 3157 (1993).
[8] C. A. Lang, M. M. Dovek, and C. F. Quate, Rev. Sci. Instrum. **60**, 3109 (1989).
[9] Robert A. Wolkow, Rev. Sci. Instrum. **63**, 4049 (1992).
[10] Kazuto Ikeda, Kenshi Takamuku, Hiroshi Kubota, Rittaporn Itti, and Naoki Koshizuka, Rev. Sci. Instrum. **64**, 2221 (1993).
[11] R. R. Schulz and C. Rossel, Rev. Sci. Instrum. **65**, 1918 (1994).
[12] Robert Wolkow, Phys. Rev. Lett. **68**, 2636 (1992).
[13] D. M. Eigler and E. K. Schwiezer, Nature **344**, 524 (1990).
[14] M. F. Crommie, C. P. Lutz, and D. M. Eigler, Science **262**, 218 (1993).
[15] S. Gwo, K.-J. Chao, C. K. Shih, K. Sadra, and B. G. Streetman, Phys. Rev. Lett. **71**, 1883 (1993).
[16] S. Gwo, K.-J. Chao, A. R. Smith, C. K. Shih, K. Sadra, and B. G. Streetman, J. Vac. Sci. Technol. B **11**, 1509 (1993).
[17] A. R. Smith, S. Gwo, K. Sadra, Y. C. Shih, B. G. Streetman, and C. K. Shih, J. Vac. Sci. Technol. B **12**, 2610 (1994).
[18] M. B. Johnson, O. Albrektsen, R. M. Feenstra, and H. W. M. Salemink, Appl. Phys. Lett. **63**, 2923 (1993).
[19] M. B. Johnson, U. Maier, H.-P. Meier, and H. W. M. Salemink, Appl. Phys. Lett. **63**, 1273 (1993).
[20] R. M. Feenstra, D. A. Collins, D. Z.-Y. Ting, M. W. Wang, and T. C. McGill, Phys. Rev. Lett. **72**, 2749 (1994).
[21] A. R. Smith, S. Gwo, and C. K. Shih, Rev. Sci. Instrum. **65**, 3216 (1994).
[22] PZT-4, PZT-5A, and PZT-5H are designations given to three PZT (lead zirconate titanate) materials by the company *Vernitron*. Their *Stavely Sensors* equivalents are referred to as EBL#1, EBL#2, and EBL#3, respectively.